Molecular Spin-Flip Loss and a Dual Quadrupole Trap

David Reens,* Hao Wu,* Tim Langen,† and Jun Ye
JILA, National Institute of Standards and Technology and the University of Colorado and Department of Physics, University of Colorado, Boulder, Colorado 80309-0440, USA
(Dated: June 5, 2017)

Doubly dipolar molecules exhibit complex internal spin-dynamics when electric and magnetic fields are both applied. Near magnetic trap minima, these spin-dynamics lead to enhancements in Majorana spin-flip transitions by many orders of magnitude relative to atoms, and are thus an important obstacle for progress in molecule trapping and cooling. The effect is strongest for Hund's case (a) states and is significant for Hund's case (b) as well. We study these internal spin-dynamics with OH molecules and devise a trap geometry where spin-flip loss can be tuned from over 200 s^{-1} to below our 2 s^{-1} vacuum limited loss rate with only a simple external bias coil and with no sacrifice of trap strength.

The ultracold regime extends toward molecules on many fronts [1]. KRb molecules have reached lattice quantum degeneracy [2] and other bialkalis continue to progress [3–6]. Creative and carefully engineered laser cooling strategies are tackling certain nearly vibrationally diagonal molecules [7–13]. A diverse array of alternative strategies have succeeded to greater or lesser extents on other molecules [14–20]. All of these molecules will require secondary strategies like evaporation or sympathetic cooling to make further gains in phase space density [21–23]. They also may face a familiar challenge: spin flip loss near the zero of a magnetic trap, but dramatically enhanced for many doubly dipolar molecules due to their internal spin dynamics in mixed electric and magnetic fields.

The knowledge of spin flips or Majorana hops as an eventual trap lifetime limit predates the very first magnetic trapping of neutrals [24]. Spin flips were directly observed near 50 μK and overcome with a time-orbiting potential trap [25] and a plugged dipole trap [26], famously enabling the first production of Bose-Einstein condensates. Motivated by the interest in dipolar molecules in mixed fields for quantum chemistry, precision measurement and many-body physics, we previously investigated loss of magnetically trapped hydroxyl radicals (OH) with applied electric field [27]. This trap loss occurred for substates of OH's $X^2\Pi_{J=3/2}$ ground state manifold other than the most well trapped one (positive parity and full spin polarization, $|f, m_J = 3/2\rangle$, blue in Fig. 1). Due to the closely spaced parity doublet, a general feature of Hund's case (a), these states intersect with opposite parity states at non-zero magnetic fields, where electric field can open avoided crossings and cause trap loss. We now identify internal spin-dynamics leading to trap loss near zero B-field even for the most well trapped state and even at 50 mK.

These internal spin-dynamics are subtle, having eluded three previous investigations of note: In [28] the analogues of atomic spin-flip loss for molecules in mixed fields were modeled, and a magnetic quadrupole trap for OH molecules with superposed electric field was specifically addressed. It was concluded that no significant loss enhancement due to electric field would be evident. This is true only for the approximate $^2\Pi_{1/2}$ Hamiltonian used in that study. In [29] E-fields were applied in our magnetic quadrupole trap to study E-field induced collisions. Although an initial approximation was made of the spin-dynamical effect, subsequent investigations have revealed it to be a threefold underestimate, enough to render deconvolution of any remaining collisional ef-

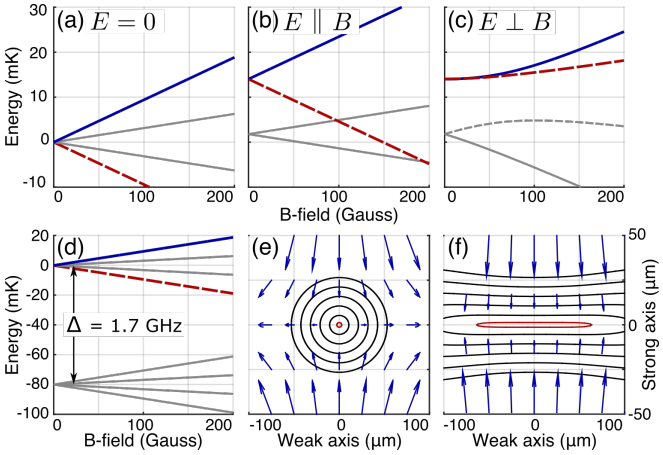

FIG. 1. A uniform E-field, added to magnetically trapped OH for dipolar studies or other purposes, can lead to spin-flip losses. Four Zeeman split lines in OH's $X^2\Pi_{3/2}$ manifold are shown (a-c), with the trapped $|f, 3/2\rangle$ state in blue and its spin-flip partner $|f, -3/2\rangle$ in dashed red. These states are shown with no E-field (a), with $E = 150$ V/cm and $E \parallel B$ (b), and with $\vec{E} \perp \vec{B}$ (c). Note the vastly reduced red-blue splitting in the latter case. The opposite parity ($|e\rangle$) manifold is split by Δ (d). Energy splitting contours are shown every 40 MHz near the zero of a 2 T/cm magnetic quadrupole trap for OH molecules [27] without E-field (e), and with uniform $E = 150$ V/cm along the strong axis of the quadrupole (f). The vectors are $\mu_B \vec{B} \pm d_E \vec{E}$, where the sign is positive above the horizontal centerline and negative below, which represents the proper quantization axis for magnetically trapped molecules. Note the drastic widening of the lowest contour (red), the culprit for molecular spin-flip loss enhancement.

fect difficult. Finally, in [30] it was correctly noted that Hund's case (a) molecules maintain a quantization axis in mixed fields. The states of the molecule were shown to align with one of the two quantization axes given by the vectors $\mu_B\vec{B} \pm d_E\vec{E}$, μ_B and d_E the effective dipole moments of the molecule in uncombined fields. It was asserted that this would maintain quantization near the zero of a quadrupole trap and avoid spin-flip loss, but as we now describe the loss is actually enhanced.

Consider a magnetic quadrupole trap, where a weak-field seeking molecule remains trapped insofar as it adiabatically follows the field direction. When molecules pass near the trap center, they experience a rotating field direction, causing spin-flips. When electric field is added, it dominates in the trap center where the magnetic field is weakest. Quantization is maintained but the quantization axis does not rotate with the magnetic field. Further away from the trap center the molecule is then magnetically strong field seeking and is lost. To avoid loss, the molecule must switch from the vector sum quantization axis to the vector difference quantization axis, so as to remain magnetically weak field seeking despite the change in relative orientation of the fields. To be more precise, we define the relative orientation of the fields as the sign of $\phi = \vec{E} \cdot \vec{B}$. When ϕ is negative (positive), the trapped state must have the vector difference (sum) quantization axis, so that an increase in magnitude of the magnetic field increases its energy. Orientation changes whenever ϕ changes sign, i.e. where $\phi = 0$ which means $\vec{E} \perp \vec{B}$. This happens in a 2D region, since $\phi = 0$ is a contour level of the 3D scalar valued function ϕ.

We can quantify this intuitive picture by diagonalizing the molecular Hamiltonian in mixed fields to find the energy splitting between the well trapped substate and its spin-flip partner (Fig. 1a-c). The preceding quantization axis discussion suggests that spin-flips occur when crossing the $\phi = 0$ planar region, so we expect to find a correspondingly reduced energy splitting there, since this splitting controls the likelihood of spin-flips along a molecule's trajectory via the Landau-Zener formula. This is indeed the case; compare panels (b-c). In fact, by series expanding the exact eigenenergies of OH, we find $H_{\vec{E}\perp\vec{B}}(B) \approx (\mu_B B)^3\Delta^2/(d_E E)^4$, Δ the lambda doubling, $B = |\vec{B}|$, and $E = |\vec{E}|$. The Zeeman splitting is no longer linear, but cubic. This means the energy splitting will be small in a much larger region surrounding the zero of a magnetic quadrupole trap than otherwise (Fig. 1e-f).

Furthermore, by comparing the flux of molecules through an energy splitting contour like those shown in Fig. 1e-f, but with the specific contour value κ for which a molecule of thermally average velocity v would flip with probability $1/e$, we can derive the scaling law for spin-flip loss enhancement $\eta \sim (d_E E/\sqrt{\kappa\Delta})^{8/3}$. So E-fields beyond $\sqrt{\kappa\Delta}/d_E$ lead to nearly cubic loss enhancements. This follows by solving $H_{\vec{E}\perp\vec{B}}(B) = \kappa$ to get the area of the contour in Fig. 1f and by solving the Landau-Zener formula $P = e^{-\kappa^2/\hbar\dot{H}} = 1/e$ to find $\kappa = \sqrt{\hbar\dot{H}}$, with $\dot{H} = 2\mu_B B' v$ the rate of approach of approach of energy levels and B' the trap gradient. For OH at 50 mK in our 2 T/cm trap [31], $\kappa = 5$ MHz, an order smaller than the lowest energy contour colored red in Fig. 1e-f. We can be more precise by integrating the flux for a thermally distributed ensemble in both space and velocity (Tab. I).

TABLE I. Enhancements (η) and loss rates (Γ) for OH with typical applied fields. Zero field values are equivalent to atomic spin-flip loss. E-field is required during evaporation and spectroscopy to open avoided crossings for $|e\rangle$ parity states [22, 27]. Background loss is 2 s^{-1}, experiment length 100 ms.

E (V/cm)	55 mK		5 mK		Purpose
	η	$\Gamma\,(s^{-1})$	η	$\Gamma\,(s^{-1})$	
0	1	0.02	1	1.3	Zero Field
300	5	0.1	9	11	Evaporation
550	17	0.3	40	50	Spectroscopy
3000	1000	19	1600	2000	Polarizing

Generalizing beyond OH, Hund's case (a) states exhibit reduced Zeeman splittings near $B = 0$ when $\vec{E} \perp \vec{B}$ that are not always cubic as for OH but satisfy $H_{\vec{E}\perp\vec{B}}(B) \propto (\mu_B B)^{2m_J}$. Only states with $m_J = 1/2$ retain a linear Zeeman splitting, but they are either not well trapped if $J = 1/2$ also, or they are initially linear until avoided crossings with other states (c.f. $|f, 1/2\rangle$ for OH, gray close dashes, Fig. 1c). This bears out in all test Hamiltonians we have diagonalized, and can be understood intuitively as follows: the Zeeman effect is a perturbation on a Hamiltonian whose quantization axis, which defines the $|m_J\rangle$ quantum number, has already been set by the Stark effect. Normally the Zeeman effect would linearly split states according to $|m_J\rangle$, but from its perspective the states are superpositions $|m_J\rangle \pm |-m_J\rangle$ and do not split at all to first order. Only via perturbations of the eigenbasis itself does a Zeeman splitting emerge.

Generalizing beyond Hund's case (a), any state which exhibits competition between the magnetic and electric fields for the alignment of the molecule will be susceptible to this effect. One way to avoid this competition is for the fields to couple to unrelated parts of the Hamiltonian, which does happen to a limited extent for Hund's case (b) states without electron orbital angular momentum (Σ states, $\Lambda = 0$) [30]. In these states, which include most laser-cooled and bialkali molecules thus far, the electric and magnetic fields couple to rotation and spin respectively, which are only related by the spin-rotation coupling constant γ. Where the field-induced shifts are large compared with γ, they stop competing, and both lead to linear energy shifts regardless of the magnitude of the other. This means that the cross sectional area of loss

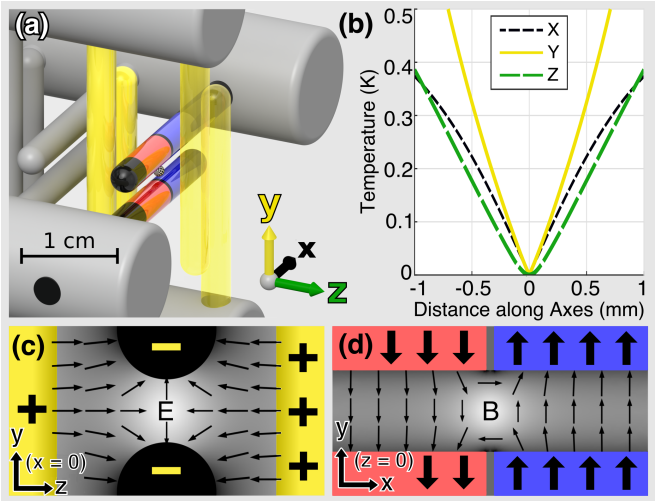

FIG. 2. The last six pins of our Stark decelerator [31] form the trap (a), which is 0.45 K deep with trap frequency $\nu \approx 4$ kHz (b). Along y the trap is bounded by the 2 mm pin spacing. The yellow pins are positively charged and the central pin pair negatively, which forms a 2D electric quadrupole trap with zero along the x-axis. This is shown for the $x = 0$ plane (c), with yellow pins artificially projected for clarity since they don't actually intersect the plane. The central pins are magnetized, with two domains each. Blue indicates magnetization along $+\hat{y}$, red along $-\hat{y}$. These domains produce a magnetic quadrupole trap with zero along the z-axis, shown in the $z = 0$ plane (d).

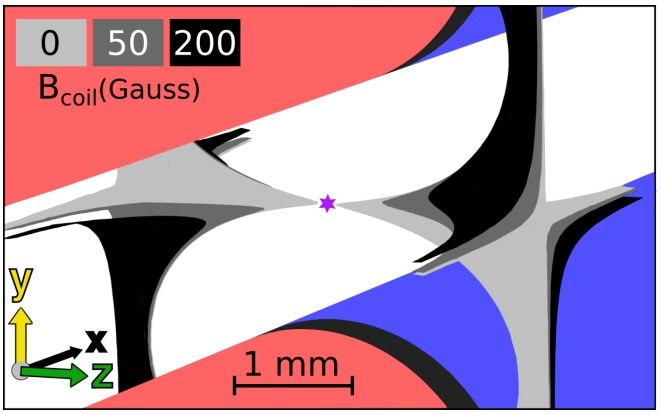

FIG. 3. Surfaces where spin-flips can occur ($\vec{E} \perp \vec{B}$, $\mu_B B < d_E E$) are shown for three values of B_{coil} in light gray, dark gray, and black. The magnetic pins are shown as in Fig. 2 for context. The purple star marks the trap center, to which molecules are confined within a ~1 mm diameter.

regions is enhanced by $(\gamma/\kappa)^2$ but is then bounded. Typical molecules have γ in the tens of MHz [23], and κ much lower than the 5 MHz for our warm and very tightly confined OH; so spin-flip loss enhancement remains important. In some cases, e.g. for YO [32], the loss can be supressed for certain hyperfine states. These states are characterized by significant electron-spin-to-nuclear-spin dipolar coupling, which results in gaps that protect them from spin-flips.

We can generalize to arbitrary geometries and consider methods to suppress the loss using a simple strategy: avoid $\mu_B B < d_E E$ where $\vec{E} \perp \vec{B}$. One way to achieve this is to trap with E-field and superpose B-field. The lambda doublet prevents flips in this configuration, but it correspondingly rounds the trap minimum, weakening confinement. Another option is to trap with both fields and keep zeros overlapped. This was once realized for OH with a superposed magnetic quadrupole and electric hexapole [33]. Such a scheme prevents spin-flip loss enhancement, but does not remove it entirely. It is also susceptible to misalignment induced loss enhancement. Another possibility is to use one field only, but any experiment which aims to make use of the doubly dipolar nature of molecules cannot accept this compromise.

We opt for a new geometry: a pair of 2D quadrupole traps, one magnetic and the other electric, with orthogonal centerlines (Fig. 2). We achieve these fields in a geometry that matches our Stark decelerator [16]. This approach is similar to the Ioffe-Pritchard strategy [34], where a 2D magnetic quadrupole is combined with an axial magnetic dipole trap. While this successfully prevents spin-flip loss, axial and radial trapping interfere, resulting in significantly lower trap depths than for a 3D quadrupole. We thwart this interference by using electric field for the third direction. Our geometry has $\vec{E} \perp \vec{B}$ in the two planes $x \cdot y = 0$, and $\mu_B B < d_E E$ in a large cylinder surrounding the z-axis. However, by adding magnetic field $\vec{B} = B_{\text{coil}}\hat{z}$ along the centerline of the magnetic quadrupole with an external bias coil, a fully tunable scenario emerges.

Adding B_{coil} only slightly rounds the magnetic trapping potential, but it morphs the $\vec{E} \perp \vec{B}$ surface from a pair of planes into a hyperbolic sheet ($x \cdot y = z \cdot B_{\text{coil}}/B'$), pushing it away from the z-axis where the magnetic field is smallest. Thus, small magnitudes of B_{coil} are sufficient to avoid loss. In Fig. 3, the surfaces where $\vec{E} \perp \vec{B}$ for several B_{coil} magnitudes are shown wherever the splitting is below the hopping threshold κ. The loss regions are always visible, but they are tuned too far away from the trap center for molecules to access. The striking difference in molecule trap lifetime with and without B_{coil} can be seen in Fig. 4a.

As a further confirmation of our model of the loss, we translate the magnetic pins along the $\hat{x}$ direction in their mounts to alter the surface where $\vec{E} \perp \vec{B}$, and compare experimental data against expectations (Fig. 4b). Qualitatively, this translation serves to disrupt the idealized 2D magnetic quadrupole by adding a small trapping field $\vec{B} \propto B' z \hat{z}$. This means that B_{coil} no longer directly tunes the magnetic field magnitude along the z-axis. Instead, B_{coil} must first overcome the slight trapping field, translating a point of zero field along the z-axis and eventually out of the trap. The point of zero magnetic field has

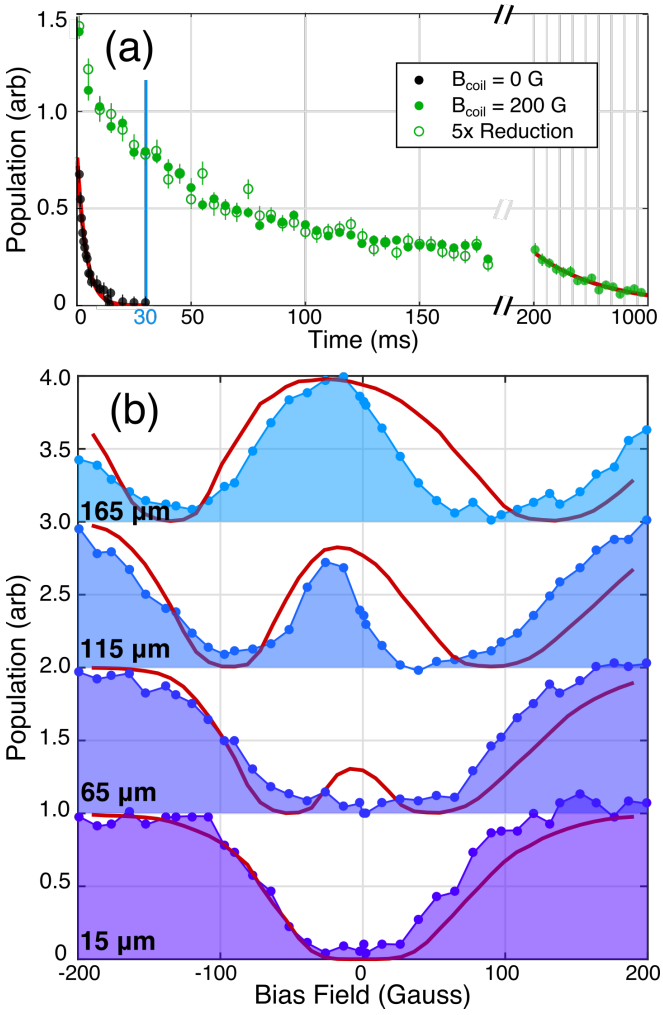

FIG. 4. Time traces (a) without bias field (black), with bias field (green dots), and with modulated density (green circles). One body fits (red) give loss rates of 200 s^{-1} without bias field and 2 s^{-1} with full bias field at long times, in agreement with our background gas pressure. At the fixed time 30 ms, population is shown as a function of both pin translation and bias field (b), for several values of pin translation, labeled relative to perfect alignment. Fits (red) are calculated by integrating the molecule flux of a thermal ensemble through surfaces where $\vec{E} \perp \vec{B}$.

$\mu_B B < d_E E$ and lies on the $\phi = \vec{E} \cdot \vec{B} = 0$ surface by definition, leading to strong loss unless it is aligned with the trap center, where E is also zero. This means that without $B_{\rm coil}$, the loss should actually be a local minimum; as $|B_{\rm coil}|$ is increased the loss should first worsen and then improve when the zero leaves the trap. This qualitative explanation matches the observed double well structure in population verses $B_{\rm coil}$.

Quantitatively, we fit the family of curves (red, Fig. 4b) by assuming a completely time independent and thermal population distribution and integrating molecule flux weighted by Landau-Zener probability over the contorted surfaces where $\vec{E} \perp \vec{B}$ for each $B_{\rm coil}$ and pin translation.

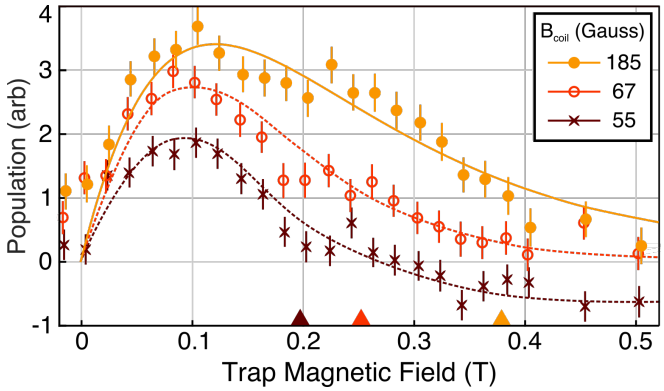

FIG. 5. Microwave spectroscopy shows that increasing $B_{\rm coil}$ increases population and shifts its distribution to higher energy. Triangles indicate the field at which a molecule can access loss regions for a given $B_{\rm coil}$. The dotted lines are eye-guides, but the solid line for highest $B_{\rm coil}$ is a fit to 175 ± 15 mK.

This idealized integral computation nonetheless matches the data with only temperature as a free parameter [35]. The fitted temperature is 170 ± 20 mK.

We further confirm our model using microwave spectroscopy (Fig. 5), which detects the molecules experiencing a specific magnetic field by transferring them to an opposite parity state that is dark to our detection laser, as in [22]. Although the magnetic energy is only part of the total energy of molecules in our dual electric and magnetic quadrupole, molecules with a high magnetic energy during our spectroscopic snapshot are more likely to have a high total energy. It is seen that increasing $B_{\rm coil}$ increases population first at low fields and then at higher fields. This is consistent with our calculations showing that loss location moves further from the trap center with increasing $B_{\rm coil}$ (Fig. 3), and thus can be accessed only by higher energy molecules. At largest $B_{\rm coil}$ the distribution fits to 175 ± 15 mK, agreeing with the pin translation fits (Fig. 4b).

In the case of lowest applied magnetic field in Fig. 5, a negative signal is observed. This indicates a build-up in a negative parity ($|e\rangle$) state. Although the spin-flips we have discussed connect $|f, 3/2\rangle$ to $|f, -3/2\rangle$, the latter experiences various avoided crossings due to the large electric confinement fields and remains weakly trapped. Its field-dressed state character varies, transitioning to $|e, 3/2\rangle$ at larger magnetic fields (Fig. 1d).

With loss removed, we observe a population trend whose initially fast decay rate decreases over time (Fig. 4a, green dots), suggestive of collisions. To test this, we implement a five-fold reduction in initial population [36] and scale the resulting trend by five (green circles). If collisions had contributed, this new trend would show less decay, but we observe no significant change. This absence of collisions differs from our earlier work [22], which as we have mentioned shows signatures

of evaporation for shallow cuts. This could be attributed to a significantly higher initial temperature and correspondingly lower density, reduced molecule number, or differences in trap geometry and loading. An alternative hypothesis for the population trend is the existence of chaotic trap orbits with long escape times [37]. Moving forward, we aim to increase the density by means of several improvements [38, 39].

Molecule enhanced spin-flip loss arises in mixed electric and magnetic fields due to a competition between field quantization axes where $\vec{E} \perp \vec{B}$ and $\mu_B B < d_E E$. We conclusively demonstrate this effect and overcome it using our dual magnetic and electric quadrupole trap. Our explanation of the effect provides detailed predictions of how its location and magnitude ought to scale with bias field and trap alignment, which we experimentally verify. Our results correct existing predictions about molecular spin-flips in mixed fields and pave the way toward further improvements in molecule trapping and cooling.

We acknowledge the Gordon and Betty Moore Foundation, the ARO-MURI, JILA PFC, and NIST for their financial support. T.L. acknowledges support from the Alexander von Humboldt Foundation through a Feodor Lynen Fellowship. We thank J.L. Bohn and S.Y.T. van de Meerakker for helpful discussions. We thank Goulven Quéméner for his continued involvement in this research.

* Contributed equally. Email dave.reens@colorado.edu or hao.wu@colorado.edu.

† Present Address: 5. Physikalisches Institut and Center for Integrated Quantum Science and Technology (IQST), Universität Stuttgart, Pfaffenwaldring 57, 70569 Stuttgart, Germany

[1] L. D. Carr, D. DeMille, R. V. Krems, and J. Ye, New Journal of Physics **11**, 055049 (2009).

[2] S. A. Moses, J. P. Covey, M. T. Miecnikowski, B. Yan, B. Gadway, J. Ye, and D. S. Jin, Science **350**, 659 (2015).

[3] T. Takekoshi, L. Reichsöllner, A. Schindewolf, J. M. Hutson, C. R. Le Sueur, O. Dulieu, F. Ferlaino, R. Grimm, and H.-C. Nägerl, Physical Review Letters **113**, 205301 (2014).

[4] J. W. Park, S. A. Will, and M. W. Zwierlein, Physical Review Letters **114**, 205302 (2015).

[5] M. Guo, B. Zhu, B. Lu, X. Ye, F. Wang, R. Vexiau, N. Bouloufa-Maafa, G. Quéméner, O. Dulieu, and D. Wang, Physical Review Letters **116**, 205303 (2016).

[6] L. R. Liu, J. T. Zhang, Y. Yu, N. R. Hutzler, Y. Liu, T. Rosenband, and K.-K. Ni, (2017), arXiv:1701.03121.

[7] B. K. Stuhl, B. C. Sawyer, D. Wang, and J. Ye, Physical Review Letters **101**, 243002 (2008).

[8] E. S. Shuman, J. F. Barry, and D. DeMille, Nature **467**, 820 (2010).

[9] M. T. Hummon, M. Yeo, B. K. Stuhl, A. L. Collopy, Y. Xia, and J. Ye, Physical Review Letters **110**, 143001 (2013).

[10] J. F. Barry, D. J. McCarron, E. B. Norrgard, M. H. Steinecker, and D. DeMille, Nature **512**, 286 (2014).

[11] V. Zhelyazkova, A. Cournol, T. E. Wall, A. Matsushima, J. J. Hudson, E. A. Hinds, M. R. Tarbutt, and B. E. Sauer, Physical Review A **89**, 053416 (2014).

[12] M. H. Steinecker, D. J. McCarron, Y. Zhu, and D. DeMille, ChemPhysChem **17**, 3664 (2016).

[13] B. Hemmerling, E. Chae, A. Ravi, L. Anderegg, G. K. Drayna, N. R. Hutzler, A. L. Collopy, J. Ye, W. Ketterle, and J. M. Doyle, Journal of Physics B: Atomic, Molecular and Optical Physics **49**, 174001 (2016).

[14] J. M. Doyle, J. D. Weinstein, R. DeCarvalho, T. Guillet, and B. Friedrich, Nature **395**, 148 (1998).

[15] H. L. Bethlem, G. Berden, and G. Meijer, Physical Review Letters **83**, 1558 (1999).

[16] J. R. Bochinski, E. R. Hudson, H. J. Lewandowski, G. Meijer, and J. Ye, Physical Review Letters **91**, 243001 (2003).

[17] E. Narevicius, A. Libson, C. G. Parthey, I. Chavez, J. Narevicius, U. Even, and M. G. Raizen, Physical Review Letters **100**, 093003 (2008).

[18] A. Wiederkehr, H. Schmutz, M. Motsch, and F. Merkt, Molecular Physics **110**, 1807 (2012).

[19] A. Prehn, M. Ibrügger, R. Glöckner, G. Rempe, and M. Zeppenfeld, Physical Review Letters **116**, 063005 (2016).

[20] Y. Liu, M. Vashishta, P. Djuricanin, S. Zhou, W. Zhong, T. Mittertreiner, D. Carty, and T. Momose, Physical Review Letters **118**, 093201 (2017).

[21] L. P. Parazzoli, N. J. Fitch, P. S. Zuchowski, J. M. Hutson, and H. J. Lewandowski, Physical Review Letters **106**, 1 (2011).

[22] B. K. Stuhl, M. T. Hummon, M. Yeo, G. Quéméner, J. L. Bohn, and J. Ye, Nature **492**, 396 (2012).

[23] G. Quéméner and J. L. Bohn, Physical Review A - Atomic, Molecular, and Optical Physics **93**, 1 (2016).

[24] A. L. Migdall, J. V. Prodan, W. D. Phillips, T. H. Bergeman, and H. J. Metcalf, Physical Review Letters **54**, 2596 (1985).

[25] W. Petrich, M. H. Anderson, J. R. Ensher, and E. A. Cornell, Physical Review Letters **74**, 3352 (1995).

[26] K. B. Davis, M. O. Mewes, M. R. Andrews, N. J. van Druten, D. S. Durfee, D. M. Kurn, and W. Ketterle, Physical Review Letters **75**, 3969 (1995).

[27] B. K. Stuhl, M. Yeo, B. C. Sawyer, M. T. Hummon, and J. Ye, Physical Review A **85**, 033427 (2012).

[28] M. Lara, B. L. Lev, and J. L. Bohn, Physical Review A **78**, 033433 (2008).

[29] B. K. Stuhl, M. Yeo, M. T. Hummon, and J. Ye, Molecular Physics **111**, 1798 (2013).

[30] J. L. Bohn and G. Quéméner, Molecular Physics **111**, 1931 (2013).

[31] B. C. Sawyer, B. K. Stuhl, D. Wang, M. Yeo, and J. Ye, Physical Review Letters **101**, 203203 (2008).

[32] This is particularly relevant given the very recently realized 3D MOT for YO.

[33] B. C. Sawyer, B. L. Lev, E. R. Hudson, B. K. Stuhl, M. Lara, J. L. Bohn, and J. Ye, Physical Review Letters **98**, 1 (2007).

[34] D. E. Pritchard, Physical Review Letters **51**, 1336 (1983).

[35] Calculation performed in COMSOL: Source Code.

[36] Microwaves couple opposite parities during deceleration, giving a uniform loss probability across the molecular distribution.

[37] R. González-Férez, M. Iñarrea, J. P. Salas, and P. Schmelcher, Physical Review E **90**, 062919 (2014).

[38] U. Even, EPJ Techniques and Instrumentation **2**, 17 (2015).
[39] Y. Segev, N. Bibelnik, N. Akerman, Y. Shagam, A. Luski, M. Karpov, J. Narevicius, and E. Narevicius, Science Advances **3**, e1602258 (2017).